Progress In Electromagnetics Research Letters, Vol. 107, 141–149, 2022

A Simple Balanced Bandpass Filter Using Loop-Type Microstrip Resonator Loaded with Shorted/Opened Stubs

Jun-Mei Yan*, Zhi-Peng Xiao, and Liang-Zu Cao

Abstract—A simple balanced bandpass filter is presented. It is constructed mainly by a loop-type resonator with loaded shorted/opened stubs. The resonator is fed by the balanced coupled-line structure. In the loop-type resonator, three approaches can be simultaneously utilized to achieve high common-mode suppression. One is that the loop-type resonator has different differential/common-mode resonant frequencies, which results in a good in-band common-mode suppression. The second is that the loaded short stubs with different lengths will make the input/output port couplings to have different coupling strengths, which will deteriorate the common-mode bandpass response. The third is that loading the grounded resistors can effectively dissipate the common-mode signal. Meanwhile, loading the grounded resistors in the balanced coupled-line structure can effectively dissipate the reflective common-mode signal. A detailed description about its structure, operational mechanism, and design method is given. For demonstration, a prototype balanced bandpass filter working at 2.4 GHz is designed, fabricated, and measured. A high in-band common-mode suppression of 49 dB is achieved. The measured and simulated results can verify the effectiveness of the proposed balanced bandpass filter and the design method.

1. INTRODUCTION

Recently, researches about balanced or differential devices have received extensive interest due to their strong immunity to environmental interference. Especially, researchers have been interested in balanced bandpass filters, and a more extensive study has been taken. The balanced bandpass filter, for the differential-mode signal, has a bandpass frequency response. However, for the common-mode signal, it must have a suppression as strong as possible.

Many approaches have been proposed to implement the differential bandpass filter. A so-called microstrip-to-slotline transition structure is utilized to realize the balanced bandpass filter [1–3]. When a differential-mode signal is inputted from two ends of the microstrip-line, the equivalent electric wall at the symmetrical position makes the microstrip-line have a virtual electrical contact with the slot-line, thus, the differential-mode signal can be transmitted from the microstrip-line to the slot-line. However, when a common-mode signal is inputted, the equivalent magnetic wall makes the microstrip-line electrically isolated with the slot-line, thus, the common-mode signal cannot be transmitted from the microstrip-line to the slot-line. So the differential-mode signals are transmitted while the common-mode ones are suppressed. Ref. [4] adopted a similar structure with the microstrip-to-slotline transition.

In [5], a so-called planar differential microstrip-pin feed structure is used as the external coupling structure of a SIW cavity. When the common-mode signal is excited, the equivalent magnetic wall will suppress SIW cavity's resonance. However, when the differential-mode signal is excited, the equivalent electric wall does not affect SIW cavity's resonance. So the differential-mode bandpass filtering response and common-mode suppression can be realized. A similar structure exists in [6, 7], where two SIW

Received 2 August 2022, Accepted 27 October 2022, Scheduled 14 November 2022
* Corresponding author: Jun-Mei Yan (yjmzhy@163.com).
The authors are with School of Mechanical and Electronic Enginerring, Jingdezhen Ceramic Institute, China.

cavities with a common ground are used. A aperture is etched on the common ground. For differential-mode excitation, the etched aperture is a equivalent electric wall and does not affect SIW cavity's resonance. For common-mode excitation, the aperture is an equivalent magnetic wall and will destruct SIW cavity's resonance.

The degenerate modes of a SIW cavity have a different field distribution, which is utilized to realize balanced bandpass filter [8]. The internal-coupling aperture is etched on the location where a strong electric field distribution exists when differential-mode signal is excited, while a weak field distribution exists when common-mode signal is excited. Thus, for the differential-mode signal, a bandpass frequency response can be realized due to a proper inter-resonator coupling. However, for the common-mode signal, a weak inter-resonator coupling exists, which will lead to the destruction of bandpass frequency response.

The above mentioned methods all involve multi-layer structure, which means a complicated fabrication process. The following methods only involve a single-layer structure.

The microstrip-line resonator has different odd/even-mode resonant frequencies, which is utilized to realize balanced bandpass filter [9, 10]. Although both differential- and common-mode signals have bandpass filtering frequency response, their central frequencies are different. So in the interested band, the differential-mode signal is transmitted, and the common-mode signal is suppressed because passband of the common-mode signal can be designed out of the interested band. For further suppression of out-of-band common-mode signal, many measures have been proposed [11–13]. The grounded resistors are introduced at the symmetrical position of the microstrip resonator [11]. The grounded resistors have no effect on differential-mode signal because the symmetrical position is the equivalent ground, and there is no current in the grounded resistors. However, for the common-mode signal, the symmetrical position is open, and there is current in the grounded resistors, thus, the common-mode signal is dissipated. Reference [12] loads microstrip stubs with different lengths at the symmetrical position of microstrip resonators. These loaded microstrip stubs only change the even-mode resonant frequencies. Thus, for common-mode excitation, the microstrip resonators have different even-mode resonant frequencies, and passband of the common-mode signal is suppressed. The approach is named as different-frequency technique.

The balanced coupled-line structure is used as the feeding structure [14, 15]. For differential-mode signal, the feeding structure is the so-called doubly short-ended coupled-line which will exhibit as a bandpass coupled-line. However for common-mode signal, the feeding structure is the so-called singly short-ended coupled-line which will exhibit as a all-stop coupled-line [14]. Further, the balanced coupled-line structure is loaded with a SIR (Stepped Impedance Resonator) at its symmetrical position [15]. The loaded SIR can generate transmission zeroes which can suppress the common-mode signal, thus producing good in-band common-mode signal attenuation.

This letter proposes a simple balanced bandpass filter. Its novelty lies in its convenience that three kinds of approaches are combined to suppress the common-mode signal. The following parts will give a detailed description about its geometry configuration, how to design differential-mode bandpass filtering response, operational mechanism of the common-mode signal suppression, etc.

2. STRUCTURE

Figure 1 gives the geometry configuration of the proposed balanced bandpass filter. It consists of a loop-type microstrip resonator and two pairs of balanced ports. The loop-type resonator is loaded with two shorted stubs (L_9, L_{10}) and two open stubs (L_6, L_7). The resonator is fed using a balanced coupled-line structure. Additionally, four lumped resistors (R_1, R_2) are loaded in the balanced bandpass filter. The loaded resistors can improve the common-mode suppression effectively, which will be illustrated in the following parts.

The balanced bandpass filter has a symmetrical geometry configuration. Perhaps the odd-even-mode method can be utilized to give a deeper understanding on it. For the differential-mode excitation, the symmetrical plane AA' is an equivalent electric wall, and the midpoints of the structure are all grounded. Thus the bisected differential-mode circuit is depicted in Figure 2 (the loaded open stubs and lumped resistors are ignored). It can be observed that the differential-mode circuit is a bandpass filter consisting of a microstrip resonator with two ends grounded and loaded with a shorted stub at its

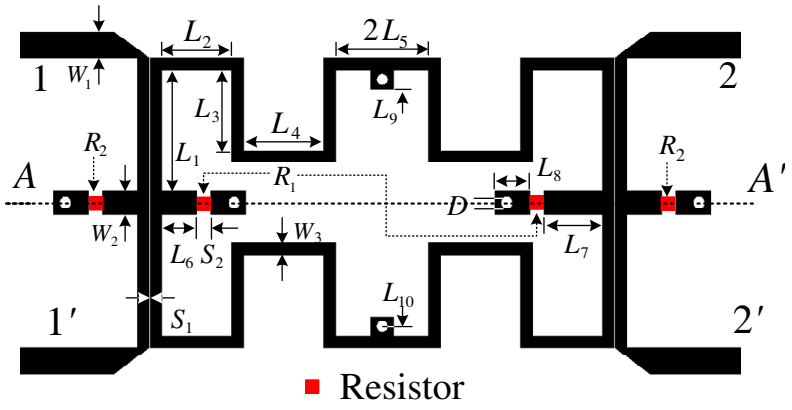

Figure 1. Layout of the proposed balanced bandpass filter.

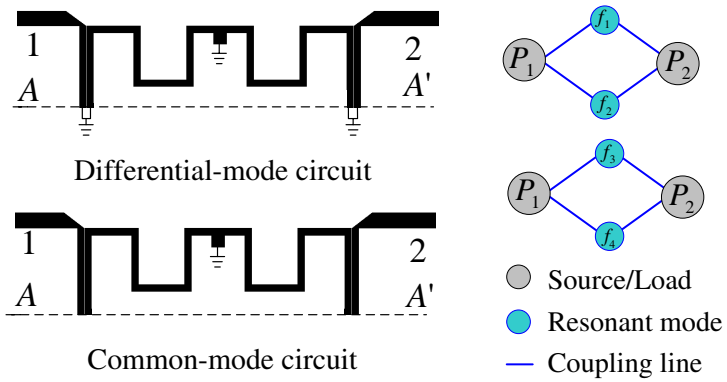

Figure 2. Diffferential/common-mode circuits and their corresponding coupling scheme (the loaded opened stubs and lumped resistors are ignored).

central position. Its coupling scheme is also included in Figure 2. The external coupling is accomplished by a shorted parallel coupling microstrip line. Correspondingly, for the common-mode excitation, the symmetrical plane AA' is an equivalent magnetic wall, and the midpoints of the structure are all open. Thus, the bisected common-mode circuit is also depicted in Figure 2 (the loaded opened stubs and lumped resistors are also ignored). It can be observed that the common-mode circuit is also a bandpass filter consisting of a half-wavelength microstrip resonator with two ends open and loaded with a shorted stub at its central position. Its coupling scheme is also included in Figure 2. The external coupling is accomplished by an open parallel coupling microstrip-line.

3. RESONANT ANALYSIS

To find resonant frequencies of the loop-type resonator, it is alone depicted in Figure 3(a) (the loaded open stubs and lumped resistors are ignored). Its odd/even-mode circuits are included in Figures 3(b) and (c). Obviously, the odd/even-mode circuits are symmetrical intrinsically. Thus the odd-even-mode method is again used to accomplish the resonant analysis. The corresponding odd/even-mode circuits are given in Figures 3(d)–(g).

From Figures 3(d)–(e), the resonators are shorted at its both ends, thus the following formulae may be used to determine the resonant frequencies when differential-mode excitation (named as differential-mode resonant frequency) is given.

$$f_{o,n}^{d} = \frac{c}{4L\sqrt{\varepsilon_e}} \cdot 2n, \quad f_{e,n}^{d} = \frac{c}{4(L+L_S)\sqrt{\varepsilon_e}} \cdot 2n \tag{1}$$

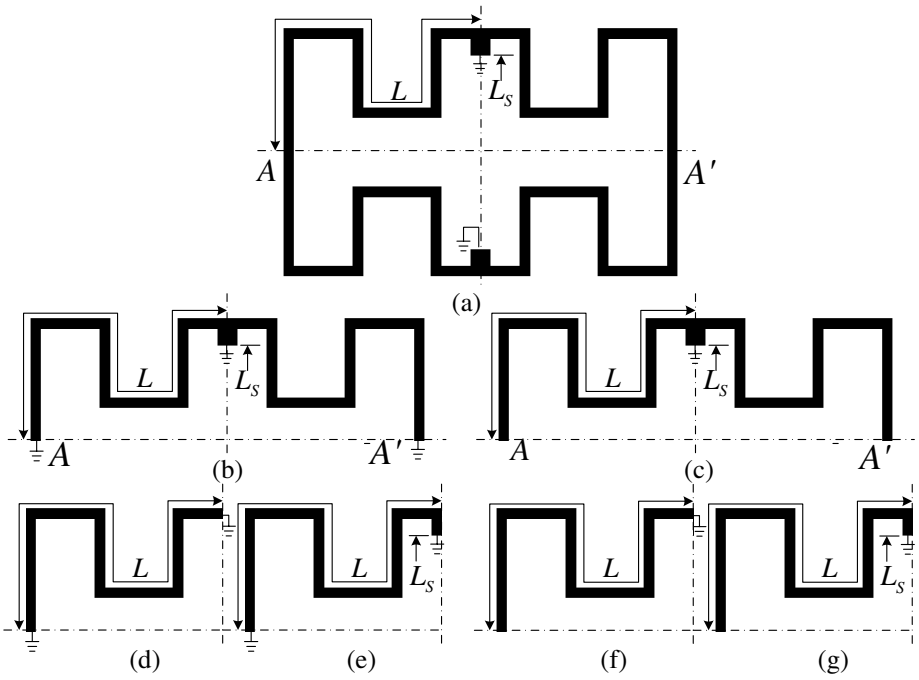

Figure 3. (a) Loop-type resonator and (b) its odd-mode bisection and (c) even-mode bisection, (d) further odd-odd-mode section, (e) odd-even-mode section, (f) even-odd-mode section and (g) even-even-mode section.

where $f^d_{o,n}$, $f^d_{e,n}$ represent odd/even-mode resonant frequency when differential-mode excitation is given; c is the light velocity in free space; and ε_e is the effective relative permittivity given by

$$\varepsilon_e = \frac{\varepsilon_r + 1}{2} + \frac{\varepsilon_r - 1}{2} \cdot \frac{1}{\sqrt{1 + 12 \cdot \frac{h}{w}}} \tag{2}$$

where h is the thickness of substrate, and w is the width of microstrip line. ε_r is the relative permittivity. When $n = 1$, the resonant mode is called as fundamental resonant mode, which is used to form the passband of the differential-mode signal. For other resonant modes, their forming passband is called parasitic passband which should be rejected as highly as possible.

From Figures 3(f)–(g), the resonators are shorted at one end and open at the other end, thus the following formulae may be used to determine the resonant frequencies when common-mode excitation (named as common-mode resonant frequency) is given

$$f^c_{o,n} = \frac{c}{4L\sqrt{\varepsilon_e}} \cdot (2n-1), \quad f^c_{e,n} = \frac{c}{4(L+L_S)\sqrt{\varepsilon_e}} \cdot (2n-1), \quad n = 1, 2, 3, \ldots \tag{3}$$

where $f^c_{o,n}$, $f^c_{e,n}$ represent odd/even-mode resonant frequencies when common-mode excitation is given. These resonant modes will form the passbands of common-mode signal, which should be rejected as much as possible.

If $f_{01} = \frac{c}{4L\sqrt{\varepsilon_e}}$, $f_{02} = \frac{c}{4(L+L_S)\sqrt{\varepsilon_e}}$, the resonant frequencies against various n are listed in Table 1. If f_{01}, f_{02} are called as the fundamental frequency, it can be found that differential-mode resonant frequencies are even-times of the fundamental frequency, and common-mode resonant frequencies are odd-times of the fundamental frequency. Thus, the differential/common-mode resonant frequencies are alternately placed, which make the passbands of differential/common-mode signals separated.

4. DESIGN OF BANDPASS FILTER FOR DIFFERENTIAL-MODE SIGNAL

Just as depicted in Figure 2, the differential-mode circuit is a second-order bandpass filter. The corresponding differential-mode resonator depicted in Figure 3 has two resonant modes which form

Table 1. Listing of resonant frequencies against various n.

n	$f^c_{o,n}$	$f^c_{e,n}$	$f^d_{o,n}$	$f^d_{e,n}$
1	f_{01}	f_{02}	$2f_{01}$	$2f_{02}$
2	$3f_{01}$	$3f_{02}$	$4f_{01}$	$4f_{02}$
⋮	⋮	⋮	⋮	⋮
n	$(2n-1)f_{01}$	$(2n-1)f_{02}$	$2nf_{01}$	$2nf_{02}$
⋮	⋮	⋮	⋮	⋮

$f_{01} = \frac{c}{4L\sqrt{\varepsilon_e}}$, $f_{02} = \frac{c}{4(L+L_S)\sqrt{\varepsilon_e}}$

the passband of the differential-mode signal. Its coupling scheme is shown in Figure 2. A rough design method modified from the conventional bandpass filter design method based on coupling coefficients [16] can be used to find an initial dimensions. The design steps are as follows. Firstly, element values g_0, g_1, g_2, g_3 of the prototype low-pass filter are obtained based on return loss and order number. Secondly, the external quality factors and internal coupling coefficient can be calculated according to the following formulae,

$$Q_{e1} = \frac{g_0 g_1}{FBW}, \quad Q_{e2} = \frac{g_2 g_3}{FBW} \tag{4}$$

$$M_{1,2} = \frac{FBW}{\sqrt{g_1 g_2}} \tag{5}$$

where FBW is the fractional bandwidth. For example, for a second-order bandpass filter with return loss of 20 dB and FBW of 2%, its low-pass elements values are $g_0 = 1.0$, $g_1 = 0.667$, $g_2 = 0.5455$, $g_3 = 1.222$, and the port quality factors and inter-resonators coupling coefficient are $Q_{e1} = Q_{e2} = 22.0$, $M_{12} = 0.0332$. The next design steps will be different from the conventional design method. Thirdly, the resonant frequencies f_1, f_2 can be obtained according to the following formulae,

$$f_1 = \sqrt{f_0^2 \cdot FBW \cdot (1 + 1/M_{12})}, \quad f_2 = \sqrt{f_0^2 \cdot FBW(1 - 1/M_{12})} \tag{6}$$

where f_0 is the center frequency. Formula (6) is derived in appendix. Fourthly, values L and L_S can be calculated by the following formulae,

$$L = \frac{c}{2\sqrt{\varepsilon_e}} \cdot \frac{1}{f_1}, \quad L_S = \frac{c}{2\sqrt{\varepsilon_e}} \cdot \left(\frac{1}{f_2} - \frac{1}{f_1}\right) \tag{7}$$

The last step is to determine the width of coupling gap S_1. Generally, a narrower gap will generate a stronger external coupling and also means a smaller quality factor. Its extraction can be done according to the following formula [16]

$$Q = \frac{\omega_0 \tau}{4} \tag{8}$$

where ω_0 is the resonant angular frequency, and τ is the group delay at ω_0. Thus, the width of the coupling gap S_1 can be determined from the extraction process based on the aimed quality factor in step 2. It should be noted that the external coupling is accomplished by the shorted parallel microstrip line. Its electrical length is chosen to be $\pi/2$ at $2f_0$, which will suppress the parasitic passband at $2f_0$ because the electric and magnetic couplings of the parallel coupling microstrip line are equal when its electric length is $\pi/2$ [17].

The above design steps are merely to determine the initial geometry dimensions. A total simulation combined with tuning works is needed to find the final design results. Figure 4(a) gives the simulated results of the designed balanced bandpass filter (HFSS 15.0 is used as the field simulation tool. Two open stubs (L_6, L_7) and the grounded resistors (R_1, R_2) are not loaded). It can be observed that, for differential-mode signal, the center frequency is at 2.4 GHz. Just as discussed in above paragraph, the first parasitic passband at double frequency is suppressed, which broadens the upper stopband. It

can also be observed that the filter has a good in-band suppression of the common-mode signal up to 48 dB. However, for the common-mode signal, several out-of-band passbands exist. The next section will discuss how to suppress the common-mode signal passbands.

5. SUPPRESSION OF COMMON-MODE SIGNAL

The first method to suppress the common-mode signal is to load two open stubs with different lengths at the symmetrical position of the loop-type resonator. The loaded stubs would not affect the bandpass filtering response of the differential-mode signal, but it will shift down the center frequencies of the common-mode signal passbands. Figure 4(b) gives the simulated results against various open stubs with different lengths. It can be clearly observed that a larger frequency-down-shift exists when a longer stub is loaded. When the two stubs have different lengths, they show a better suppression ability on the common-mode signal. Why is that? The reason is that the loaded open stubs with different lengths would make the input/output coupling to have different coupling strengths, which will destruct the passband. The second method is to load the lumped resistors at the end of the open stubs, just as depicted by R_1 in Figure 1. The loaded resistors would not affect the bandpass filtering response of the differential-mode signal, but they can suppress the common-mode signal obviously. Figure 4(c) gives the simulated results against different impedance values. It can be observed that a high common-mode suppression of up to 25 dB over the whole band is obtained.

Additionally, by loading the lumped resistors at the symmetrical position of the balanced coupled-line structure, just as depicted by R_2 in Figure 1, the reflective common-mode signal can be dissipated partially. Figure 4(d) gives the simulated results when two lumped resistors are loaded. S_{11}^{dd} is less than 10 dB up to $2f_0$.

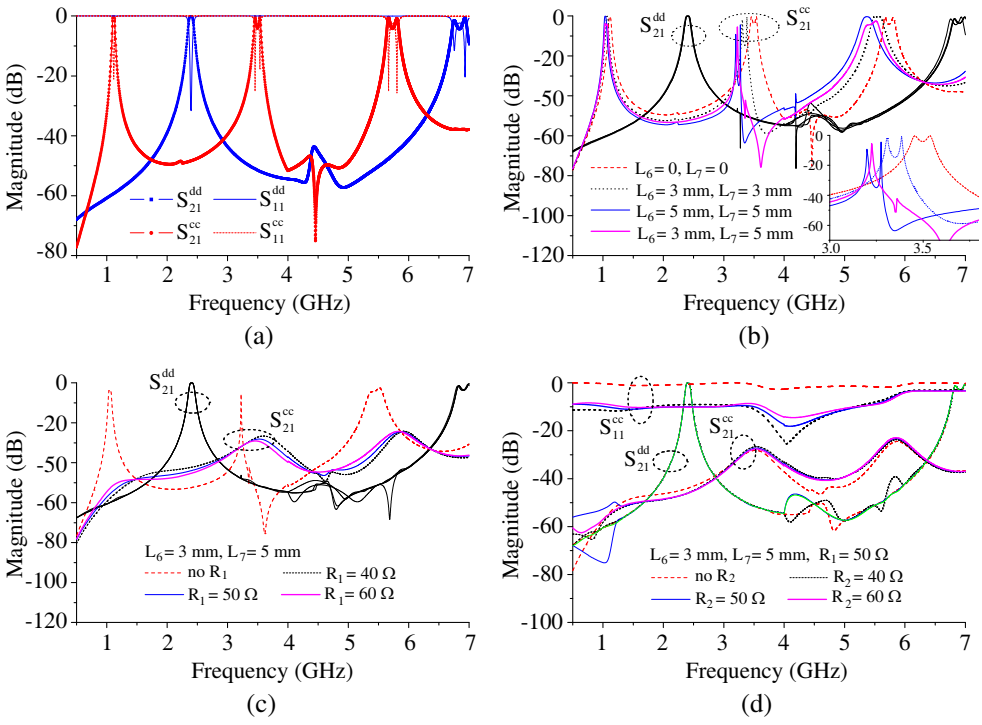

Figure 4. Simulated results against various situations: (a) no open stubs and no resistors are loaded, (b) open stubs are loaded and no resistors are loaded, (c) open stubs and two resistors are loaded with the loop-type resonator, (d) two resistors are loaded with balanced coupling line.

6. SIMULATION AND MEASUREMENT RESULTS

For verification, a prototype balanced bandpass filter with the center frequency of 2.4 GHz, FBW of 2.0%, and in-band return loss of 20 dB is designed, fabricated, and measured. The used microstrip substrate is F4B-2, and it has relative permittivity of 2.55 and thickness of 0.8 mm. HFSS 15.0 is used as the field simulation tool, and the vector network analyzer (Agilent E5071B) is used for measurement. Agilent E5071B has only two ports, and the proposed balanced bandpass filter has four ports, thus it cannot be directly measured.

The four-port scattering parameters S_{11}, S_{12}, S_{21}, S_{22}, S_{31}, S_{32}, S_{41}, and S_{42} are measured firstly using Agilent E5071B. Then these scattering parameters are transformed into the differential/common-mode scattering parameters S_{11}^{dd}, S_{21}^{dd}, S_{11}^{cc}, and S_{21}^{cc} [18]. The simulated and measured results are given in Figure 5, and a photograph of the fabricated differential bandpass filter is shown as inset. Its physical dimensions are as follows (units: mm): $S_1 = 0.1$, $S_2 = 1.2$, $W_1 = 2.2$, $W_2 = 2.0$, $W_3 = 1.0$, $L_1 = 10.5$, $L_2 = 6.0$, $L_3 = 7.0$, $L_4 = 6.9$, $L_5 = 4.0$, $L_6 = 3.0$, $L_7 = 5.0$, $L_8 = 3.0$, $L_9 = 1.7$, $L_{10} = 0.9$, $D = 1.0$. The total circuits size is $29.4 \times 56.6\,\text{mm}^2$ about $0.34 \times 0.65\lambda_g^2$, where λ_g is the guided wavelength of 50 Ω microstrip line at the center frequency. For the differential-mode signal, the passband centered at 2.42 GHz can be observed. At the center frequency, the insertion/return loss is 2.0/20 dB. The upper stopband suppression of 25 dB is up to 6.8 GHz ($2.8f_0$). For the common-mode signal, the in-band suppression is high up to 49 dB, and a suppression of 25 dB for the entire measured band (0.5–7 GHz) is obtained. Additionally, it can be observed that the common-mode return loss of 6.7 dB up to 5.8 GHz is achieved. The common-mode reflective signal can be dissipated partially. It can be observed that a discrepancy between the simulated and measured results exists, and especially, a parasitic passband at about 4.7 GHz exists. The discrepancy may be attributed to the fabrication

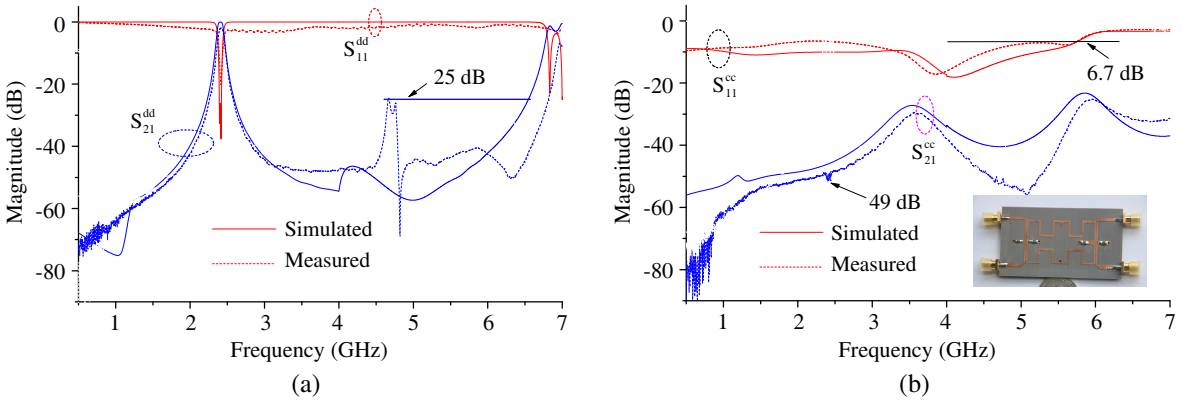

Figure 5. (a) The simulated and measured differential-mode results, (b) common-mode results and photograph of the fabricated balanced bandpass filter as inset.

Table 2. Comparison with other similar works.

	f_0^d (GHz)	IL (dB) @ f_0^d	$\lvert S_{21}^{cc}\rvert$ (dB)		Dissipation of S_{11}^{cc} (Yes/No)
			@ f_0^d	Out-of-band	
(9)	2.465	1.32	38.6	< -30 (0–5 GHz)	No
(10)	2.4	1.1	35	< -30 (0–4.3 GHz)	No
(12)	3.49	1.4	41.6	< -30 (0–8.6 GHz)	No
(13)	2.0	0.5	27.8	< -20 (0–3.8 GHz)	No
(14)	5.2	1.76	41	< -38 (0–9.0 GHz)	No
This work	2.425	2.0	49	< -25 (0–7.0 GHz)	Yes

errors, the nonuniform substrate, or the indirect measuring method. However, the measured results have a similar variation trend to the simulated results. Additionally, the measured differential-mode passband has a good agreement with simulated one. So, it can be concluded that the measured results can verify effectiveness of the proposed balanced bandpass filter and correctness of the mechanism analysis and design method. Table 2 gives a comparison with other similar works. Its remarkable advantages lie in the high in-band common-mode suppression and wideband out-of-band common-mode suppression. Additionally, the reflective common-mode signal is also dissipated partially.

7. CONCLUSIONS

A simple balanced bandpass filter using a loop-type microstrip resonator loaded with shorted/opened stubs is presented in this letter. The loop-type microstrip resonator loaded with shorted/opened stubs gives the convenience that three kinds of approaches can be combined to suppress the common-mode signal in the resonator. The geometry configuration and operation mechanism are described in detail. The conventional bandpass filter design method based on coupling coefficients can be applied to design the differential-mode bandpass filtering response approximately. The detailed design steps are given. The common-mode suppression methods are discussed. A prototype balanced bandpass filter is designed, fabricated, and measured. The simulated and measured results are given, which can verify effectiveness of the proposed balanced bandpass filter and correctness of the mechanism analysis and design method.

ACKNOWLEDGMENT

This work is supported by the National Natural Science Foundation of China (grant No. 61741110, 61661023) and in part by the Science Foundation of Education Department of Jiangxi Province.

APPENDIX A. THIS IS THE FIRST APPENDIX

In this Appendix, derivation of formula (6) is carried out. As we all known, the coupling coefficients of two uniform resonators can be extracted from the following formula [16]

$$M = \frac{f_2^2 - f_1^2}{f_2^2 + f_1^2} \tag{A1}$$

where f_2, f_1 are the transmission poles when a weak external coupling is on.

$$f_2^2 - f_1^2 = (f_2 + f_1)(f_2 - f_1) = 2f_0\Delta f = 2f_0^2 \cdot FBW \tag{A2}$$

where $FBW = \frac{2\Delta f}{f_0}$ is the fractional width and, and here, an approximation is done, i.e., f_2, f_1 are seen as the side frequencies of the passband. Thus, from Equations (A1) and (A2), the following formula

$$f_2^2 + f_1^2 = \frac{f_2^2 - f_1^2}{M} = \frac{2f_0^2 \cdot FBW}{M} \tag{A3}$$

can be obtained. From Equations (A2) and (A3),

$$f_2 = \sqrt{f_0^2 \cdot FBW \cdot (1 + 1/M)} \tag{A4}$$

$$f_1 = \sqrt{f_0^2 \cdot FBW \cdot (1 - 1/M)} \tag{A5}$$

can be obtained. Derivation ends.

Because, in fact, $f_0 \cdot FBW$ is more than $f_2 - f_1$, the obtained f_2, f_1 from Equations (A4) and (A5) shift up a little compared with the practical transmission poles.

REFERENCES

1. Ouyang, Z. A., L. Zhu, and L. L. Qiu, "Wideband balanced filters with intrinsic common-mode suppression using coplanar strip double-sided shunt-stub structures," *IEEE Trans. Microw. Theory Techn.*, Vol. 69, No. 8, 3770–3782, 2021.
2. Zhang, S., L. Qiu, and Q. Chu, "Multiband balanced filters with controllable bandwidths based on slotline coupling feed," *IEEE Microw. Wireless Compon. Lett.*, Vol. 27, No. 11, 974–976, 2017.
3. Wei, F., P. Y. Qin, Y. J. Guo, C. Ding, and X. W. Shi, "Compact balanced dual- and tri-band BPFs based on coupled complementary split-ring resonators (C-CSRR)," *IEEE Microw. Wireless Compon. Lett.*, Vol. 26, No. 2, 107–109, 2016.
4. Deng, H. W., L. Sun, Y. F. Xue, F. Liu, and T. Xu, "High selectivity and common-mode suppression balanced bandpass filter with TM dual-mode SIW cavity," *IET Microwaves, Antennas & Propagation*, Vol. 13, No. 12, 2129–2133, 2019.
5. Zhu, J.-M., H.-W. Deng, Y.-K. Han, S.-B. Xing, and W. Han, "Compact triple-mode HMSIW balanced passband filter with intrinsic common-mode suppression," *Microwave and Optical Technology Letters*, Vol. 63, No. 7, 1803–1806, 2021.
6. Deng, H. W., Y. K. Han, L. Sun, J. M. Zhu, and S. B. Xing, "Multilayer dual-mode balanced SIW filter utilizing PECCPMC characteristic for common-mode suppression," *IEEE Microw. Wireless Compon. Lett.*, Vol. 30, No. 9, 865–868, 2020.
7. Jin, C., J. X. Chen, H. Chu, and Z. H. Bao, "X-band differential bandpass filter with high common-mode suppression using substrate integrated waveguide cavity," *Electronics Letters*, Vol. 50, No. 2, 88–89, 2014.
8. Li, P., H. Chu, D. Zhao, and R. S. Chen, "Compact dual-band balanced SIW bandpass filter with improved common-mode suppression," *IEEE Microw. Wireless Compon. Lett.*, Vol. 27, No. 4, 347–349, 2017.
9. Fernández-Prieto, A., A. Lujambio, J. Martel, F. Medina, F. Mesa, and R. R. Boix, "Simple and compact balanced bandpass filters based on magnetically coupled resonators," *IEEE Trans. Microw. Theory Techn.*, Vol. 63, No. 6, 1843–1853, 2015.
10. Deng, H. W., T. Zhang, F. Liu, and T. Xu, "High selectivity and CM suppression frequency-dependent coupling balanced BPF," *IEEE Microw. Wireless Compon. Lett.*, Vol. 28, No. 5, 413–415, 2018.
11. Chen, J., M. Du, Y. Li, Y. Yang, and J. Shi, "Independently tunable/controllable differential dual-Band bandpass filters using element-loaded stepped-impedance resonators," *IEEE Transactions on Components, Packaging and Manufacturing Technology*, Vol. 8, No. 1, 113–120, 2018.
12. Lee, C. H., C. I. Hsu, H. H. Chen, and Y.-S. Lin, "Balanced single- and dual-band BPFs using ring resonators," *Progress In Electromagnetics Research*, Vol. 116, 333–346, 2011.
13. Liu, Q. J. Wang, G. Zhang, L. Zhu, and W. Wu, "A new design approach for balanced bandpass filters on right-angled isosceles triangular patch resonator," *IEEE Microw. Wireless Compon. Lett.*, Vol. 29, No. 1, 5–7, 2019.
14. Yan, T., D. Lu, J. Wang, and X. Tang, "High-selectivity balanced bandpass filter with mixed electric and magnetic coupling," *IEEE Microw. Wireless Compon. Lett.*, Vol. 26, No. 6, 398–400, 2016.
15. Yang, L., W. W. Choi, K. W. Tam, and L. Zhu, "Balanced dual-band bandpass filter with multiple transmission zeros using doubly short-ended resonator coupled line," *IEEE Trans. Microw. Theory Techn.*, Vol. 63, No. 7, 2225–2232, 2015.
16. Hong, J. S. and M. J. Lancaster, *Microstrip Filter for RF/Microwave Applications*, John Wiley & Sons, 2001.
17. Wang, H. and Q. X. Chu, "A narrow-band hairpin-comb two-pole filter with source-load coupling," *IEEE Microw. Wireless Compon. Lett.*, Vol. 20, No. 7, 372–374, 2010.
18. Bockelman, D. E. and W. R. Eisenstadt, "Combined differential and common-mode scattering parameters: theory and simulation," *IEEE Trans. Microw. Theory Techn.*, Vol. 43, No. 7, 1530–1539, 1995.